Available online at www.sciencedirect.com

SciVerse ScienceDirect

Geochimica et Cosmochimica Acta 89 (2012) 302–317

Geochimica et Cosmochimica Acta

www.elsevier.com/locate/gca

Selenium as paleo-oceanographic proxy: A first assessment

Kristen Mitchell [a,b,c,*], Paul R.D. Mason [b], Philippe Van Cappellen [c], Thomas M. Johnson [d], Benjamin C. Gill [e,f], Jeremy D. Owens [e], Julia Diaz [a], Ellery D. Ingall [a], Gert-Jan Reichart [b], Timothy W. Lyons [e]

[a] School of Earth and Atmospheric Sciences, Georgia Institute of Technology, Atlanta, GA 30332-0340, USA
[b] Department of Earth Sciences, Utrecht University, Budapestlaan 4, 3584 CD Utrecht, The Netherlands
[c] Department of Earth and Environmental Sciences, University of Waterloo, Waterloo, ON, Canada N2L 3G1
[d] Geology Department, 245 Natural History Building, MC-102, University of Illinois, Urbana-Champaign, Urbana, IL 61801, USA
[e] Department of Earth Sciences, University of California, 900 University Avenue, Riverside, CA 92521, USA
[f] Department of Earth and Planetary Sciences, Harvard University, 20 Oxford Street, Cambridge, MA 02138, USA

Received 26 October 2011; accepted in revised form 29 March 2012; available online 7 April 2012

Abstract

Selenium (Se) is an essential trace element, which, with multiple oxidation states and six stable isotopes, has been suggested as a potentially powerful paleoenvironmental proxy. In this study, bulk Se concentrations and isotopic compositions were analyzed in a suite of about 120 samples of fine-grained marine sedimentary rocks and sediments spanning the entire Phanerozoic. While the Se concentrations vary greatly (0.22–72 ppm), the $\delta^{82/76}$Se values fall in a fairly narrow range from −1 to +1‰ (relative to NIST SRM3149), with the exception of laminated black shales from the New Albany Shale formation (Late Devonian), which have $\delta^{82/76}$Se values of up to +2.20‰. Black Sea sediments (Holocene) and sedimentary rocks from the Alum Shale formation (Late Cambrian) have Se to total organic carbon ratios (Se/TOC) and $\delta^{82/76}$Se values close to those found in modern marine plankton ($1.72 \pm 0.15 \times 10^{-6}$ mol/mol and 0.42 ± 0.22‰). For the other sedimentary sequences and sediments, the Se/TOC ratios show Se enrichment relative to modern marine plankton. Additional input of isotopically light terrigenous Se may explain the Se/TOC and $\delta^{82/76}$Se data measured in recent Arabian Sea sediments (Pleistocene). The very high Se concentrations in sedimentary sequences that include the Cenomanian–Turonian Oceanic Anoxic Event (OAE) 2 may reflect an enhanced input of volcanogenic Se to the oceans. As the latter has an isotopic composition not greatly different from marine plankton, the volcanogenic source does not impart a distinct signature to the sedimentary Se isotope record. The lowest average $\delta^{82/76}$Se values are observed in the OAE2 samples from Demerara Rise and Cape Verde Basin cores ($\delta^{82/76}\text{Se} = -0.14 \pm 0.45$‰) and could reflect fractionation associated with microbial or chemical reduction of Se oxyanions in the euxinic water column. In contrast, a limiting availability of seawater Se during periods of increased organic matter production and burial may be responsible for the elevated $\delta^{82/76}$Se values and low Se/TOC ratios in the black shales of the New Albany Shale formation. Overall, our results indicate that to unlock the full proxy potential of marine sedimentary Se records, we need to gain a much more detailed understanding of the sources, chemical speciation, isotopic fractionations and cycling of Se in the marine environment.

1. INTRODUCTION AND BACKGROUND

Selenium (Se) exhibits four major oxidation states in the environment: −II, 0, +IV, and +VI. It also has six stable isotopes: ^{74}Se, ^{76}Se, ^{77}Se, ^{78}Se, ^{80}Se, and ^{82}Se. Given the multiple oxidation states and multiple isotopes, Se has the

* Corresponding author. Current address: Department of Earth and Environmental Sciences, University of Waterloo, Waterloo, ON, Canada N2L 3G1.
E-mail address: kristen.mitchell@uwaterloo.ca (K. Mitchell)

0016-7037/$ - see front matter © 2012 Elsevier Ltd. All rights reserved.
http://dx.doi.org/10.1016/j.gca.2012.03.038

potential to be a powerful paleoenvironmental proxy. Selenium isotopes have a long history among the 'non-traditional' stable isotopes, starting with the original study of Krouse and Thode (1962). Selenium isotope ratios were first measured using gas source mass spectrometry (Krouse and Thode, 1962). This technique was relatively sensitive but it required large sample quantities (>10 μg Se). The advent of the multi-collector inductively coupled plasma mass spectrometer (MC-ICP-MS) resulted in a dramatic reduction in sample sizes, enabling a wider range of applications (Rouxel et al., 2002). Although selenium isotopes are proving to be useful environmental (Johnson et al., 1999, 2000; Herbel et al., 2002; Clark and Johnson, 2008, 2010) and geological tracers (Rouxel et al., 2002, 2004; Wen et al., 2006, 2007; Zhu et al., 2008; Wen and Carignan, 2011), much work remains to be done to fully delineate the isotopic fractionations associated with the biogeochemical Se cycle (for reviews, see Johnson and Bullen (2004), and Johnson (2004)). Here, we present a first evaluation on whether Se concentrations and isotope signatures ($\delta^{82/76}$Se) in marine shales and mudstones can yield information on the prevailing environmental conditions during sediment deposition.

The biogeochemical cycle of Se is often compared to that of sulfur (S) (Zehr and Oremland, 1987; Stolz et al., 2002; Hoefs, 2009). However, while the two elements share chemical similarities, their oceanic cycles exhibit marked differences. Dissolved total Se concentrations in seawater are very low (<1 nM or <0.08 ppb, Cutter and Bruland, 1984) in contrast to the high abundance of sulfate (~28 mM). Major inputs of selenium to the ocean are atmospheric deposition (i.e., dust and volcanic ash), hydrothermal inputs, and riverine discharge (Suzuoki, 1964; Von Damm et al., 1985a,b; Auclair et al., 1987; Nriagu, 1989; Von Damm, 1991; Rouxel et al., 2002, 2004; German and Von Damm, 2003). Dissolved Se in the water column exists as Se(VI) plus Se(IV) oxyanions and as dissolved organic Se, with the latter often dominating total dissolved Se in oxic and anoxic marine waters (Cutter, 1982; Cutter and Bruland, 1984; Cutter, 1992; Baines et al., 2001). Selenium oxyanions exhibit nutrient-like depth distributions in the ocean, unlike sulfate, which behaves conservatively in the water column (Measures and Burton, 1980a,b; Measures et al., 1983; Cutter and Bruland, 1984; Cutter and Cutter, 1995; Johnson, 2004). Assimilatory uptake by plankton accounts for most of the dissolved Se removal in the surface ocean (Cutter and Bruland, 1984). Selenium is generally taken up as selenate (SeO_4^{2-}) or selenite (SeO_3^{2-}) during assimilatory reduction, although dissolved organic Se can also be directly assimilated from seawater (Baines et al., 2001).

The major supply of Se to modern marine sediments is the deposition of organic detritus at the seafloor (Wrench and Measures, 1982; Cutter and Bruland, 1984; Ohlendorf, 1989; Baines and Fisher, 2001; Böning et al., 2005; Borchers et al., 2005). Selenium in organic compounds is mainly under the –II oxidation state (Rother, 2012). Evidence from sediments collected in the NW Pacific show that Se deposited at the seafloor as organic Se remains largely bound to organic matter throughout early diagenesis (Sokolova and Pilipchuck, 1973). Organically-bound Se is also frequently the dominant form of Se in ancient shales. Kulp and Pratt (2004), for instance, determined that on average 64% of Se in shales from South Dakota and Wyoming is in the organic fraction. The other main form of Se in marine and freshwater sediments is elemental Se, which can be produced by reductive or oxidative processes in the water column or in the sediments (Cutter and Bruland, 1984; Velinsky and Cutter, 1990, 1991). Organic matter has been suggested to be the parent material of elemental Se found in carbonaceous shales (Martens and Suarez, 1997; Wen and Qiu, 1999, 2002; Zhu et al., 2004, 2008; Wen et al., 2006, 2007; Wen and Carignan, 2011).

Selenium oxyanions can be reduced via dissimilatory reduction processes, which are carried out by a number of different microbes (Oremland et al., 1989; Oremland et al., 1990; Oremland, 1991, 1994). While elemental Se is typically the predominant end-product of microbial Se reduction, Se(0) can be further reduced to selenide, Se(−II) (Herbel et al., 2003). Abiotic redox reactions also play an important role in Se cycling. For example, under sulfidic conditions selenite can reductively precipitate as elemental Se (Eq. (1)) and possibly also form polysulfidic Se and thiol-bound Se (Weres et al., 1989; Hockin and Gadd, 2003; Breynaert et al., 2008):

$$SeO_3^{2-} + 2HS^- + 4H^+ \rightarrow Se^0 + 2S^0 + 3H_2O \qquad \Delta G^\circ = -324.3\ \text{kJ/mol} \qquad (1)$$

Selenate and selenite oxyanions sorb to organic matter, iron oxides and iron sulfides (Balistrieri and Chao, 1987; Bruggeman et al., 2005; Scheinost and Charlet, 2008). Selenite, however, tends to bind far more strongly than selenate. Adsorption of selenite on pyrite (FeS_2) is followed by reduction to elemental Se (Bruggeman et al., 2005). Selenite sorbed to mackinawite (FeS) is reduced to either elemental Se or Se(−II) in the form of FeSe, depending on pH (Scheinost and Charlet, 2008). Thus, the available evidence indicates that diverse pathways may lead to burial in marine sediments of Se under the form of organic selenide, sorbed selenite, elemental Se and iron-bound selenide.

Redox transformation can fractionate the stable isotopes of Se. Reported ranges of fractionation factors (given as ε values) are summarized in the lower part of Fig. 1. The redox pathways that have been shown to produce significant Se isotope fractionation include biotic dissimilatory reduction and abiotic reduction of Se(VI) and Se(IV) oxyanions by green rust (Herbel et al., 2000, 2002; Johnson and Bullen, 2003, 2004; Ellis et al., 2003). Large isotope fractionations have also been observed in chemical reduction experiments performed under highly acidic conditions and at high temperatures (Krouse and Thode, 1962; Rees and Thode, 1966; Rashid and Krouse, 1985). Although the reduction of selenite by sulfide (Eq. (1)) could produce significant fractionations, this has yet to be demonstrated.

Isotope fractionations associated with assimilatory processes are often disregarded in stable isotope studies, because they are generally small in comparison to isotope fractionation resulting from dissimilatory processes. However, as can be seen in Fig. 1, in the Se isotope system even

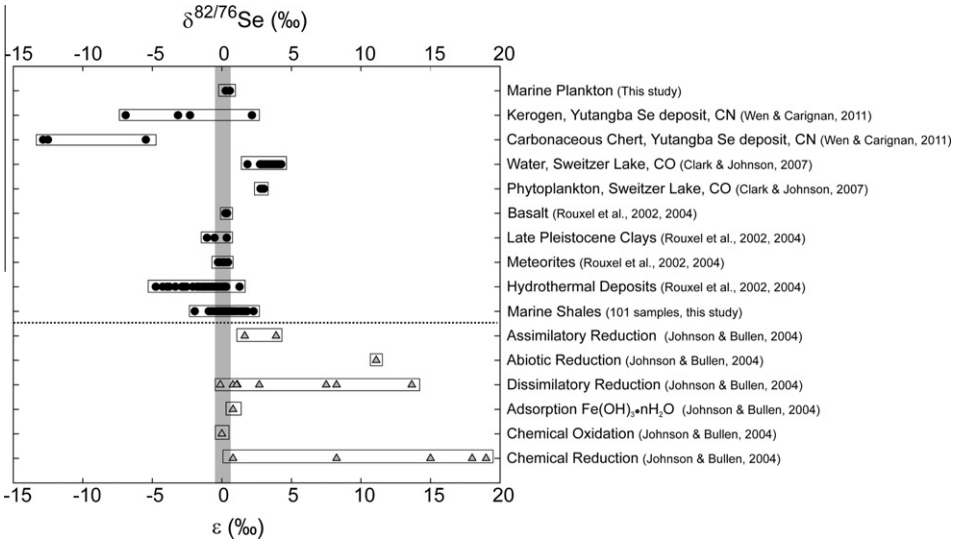

Fig. 1. Compilation of $^{82/76}$Se isotope fractionations (ε; grey triangles), and $^{82/76}$Se isotopic compositions (δ; solid circles) of natural materials, including rocks, sediments, ore deposits, plankton and natural waters. Note that the fractionations reported as $^{80/76}$Se by Johnson and Bullen (2004) are converted to $^{82/76}$Se using the relationship $\varepsilon_{80/76} = 2/3\ \varepsilon_{82/76}$.

limited fractionation during assimilatory reduction may be significant because of the fairly narrow overall range of isotope fractionation, up to 15‰ for $\varepsilon^{82/76}$Se compared to 72‰ for ε^{34}S (Tudge and Thode, 1950; Krouse and Thode, 1962; Canfield et al., 2005). In one laboratory study of algal uptake of selenate and selenite by the freshwater species *Chlamydomonas reinhardtii* $\varepsilon^{82/76}$Se values between 1.5‰ and 3.90‰ were obtained (Hagiwara, 2000).

Our study focuses on Se in well-characterized marine shale and mudstone sequences from various Phanerozoic time intervals, as well as their modern counterparts. Fine grained sediments and sedimentary rocks are selected because of their relatively high Se concentrations (Turekian and Wedepohl, 1961). The bulk Se concentrations measured in the samples analyzed in this study vary widely, from 0.22 to 72 ppm. Much higher Se concentrations have been observed in shale formations from China (Wen et al., 2007; Zhu et al., 2008; Wen and Carignan, 2011). However, these exceptional Se enrichments, which are also accompanied by wide ranges in Se isotopic composition, are clearly the result of secondary redistribution processes (Wen and Carignan, 2011) and are, therefore, excluded from our study.

The Phanerozoic sequences we analyzed all include black shale horizons. The usually high organic carbon concentrations and increased burial rates of organic carbon associated with black shales have been proposed to result from (1) increased primary productivity and/or (2) enhanced preservation of organic carbon due to anoxic conditions (Arthur et al., 1987). Generally, some combination of these two factors are thought to accompany the formation of black shale sequences, though this is still a matter of debate (Jenkyns, 2010). Increased productivity may be caused by an increase in the availability of limiting nutrients due to increased supply from the continents or more efficient nutrient recycling in the oceans (Wignall, 1994; Van Cappellen and Ingall, 1994, 1996). Enhanced respiratory oxygen demand resulting from the increased supply of organic matter may in turn enhance the expansion of anoxic bottom waters (Wignall, 1994). Because of the multiple controls on the organic matter content of marine sediments, which include but are not exclusively dependent on bottom water oxygenation, paleo-redox conditions are generally assessed using a variety of geochemical (e.g., iron speciation and trace element enrichments), sedimentological (e.g., laminations) and ecological characteristics (e.g., abundance and depth distributions of benthic organisms).

Periods of time when oxygen-depleted waters covered large areas of the seafloor are known as Oceanic Anoxic Events or OAEs. They are typically recognized by extensive black shale stratigraphic horizons transcending local basins (Schlanger and Jenkyns, 1976). Major Phanerozoic OAEs occurred during the Toarcian (~183 Ma), the Early Aptian (OAE1a; ~120 Ma), and the Cenomanian–Turonian (OAE2; ~93 Ma) (Jenkyns, 2010). Here, sedimentary sequences that comprise the following three OAEs are investigated: OAE2, the Toarcian OAE and the Steptoean Positive Carbon Isotope Excursion or SPICE. Also included in this study are samples from the New Albany Shale (Devonian–Mississippian) that were deposited under oscillating bottom water redox conditions, as well as modern sediments from the anoxic-sulfidic (euxinic) Black Sea and oxic to suboxic Arabian Sea. The data are used to assess to what extent Se concentrations and $\delta^{82/76}$Se stable isotope ratios reflect (paleo-)depositional conditions, including redox conditions at the seafloor.

2. MATERIALS

2.1. Marine plankton

A plankton sample was obtained from the oligotrophic central North Pacific Ocean (138.9999°W, 32.0002°N) using a plankton net with a mesh size of 200 μm on board *R/V*

Kilo Moana in July 2008. The sample consists of 10–15% zooplankton, with phytoplankton making up the remainder, including but not limited to *Trichodesmium sp*., *Hemiaulus sp.* and *Ethmodiscus sp.* (Watkins-Brandt, 2010; Brzezinski et al., 2011; Fujieki et al., 2011). The sample was freeze-dried, split into two separate sub-samples of equal weight. The two sub-samples were processed following the same procedures as the sediment and rock samples (described below).

2.2. Black Sea: modern euxinic basin

The Black Sea is the largest existing euxinic basin and serves as an analog for ancient deposition and preservation of organic matter under euxinic conditions (Lyons and Kashgarian, 2005). The Black Sea represents a quasi-steady state system with anoxic deep-water replacement times on the order of 2000 years. Numerous geochemical proxies have been validated in the Black Sea, including reactive plus total iron concentrations and the degree of pyritization (Canfield et al., 1996; Raiswell and Canfield, 1998; Lyons and Kashgarian, 2005), molecular biomarkers (Sinninghe Damsté et al., 1993), and molybdenum isotopes (Arnold et al., 2004).

Black Sea sediments were collected during Leg 4 of the 1988 *R/V Knorr* Black Sea Oceanographic Expedition using a box corer (Lyons, 1991; Lyons et al., 1993). Sediments from stations 3, 4, 9, 14 and 16 were analyzed in this study. Samples from station 9 and 14 contain unit 1 (non-turbidite) sediments (Degens and Ross, 1974). Stations 3 and 4 are located west of the Bosporus, Station 16 is in the Bay of Sinop. For detailed site and sedimentological descriptions, see Lyons (1991). Sediments deposited under oxic bottom waters have total organic carbon (TOC) contents of ~1 wt.%, those from the deep anoxic (euxinic) basin have significantly higher TOC contents of around 5 wt.%. The sediments are all of Holocene age.

2.3. Arabian Sea: modern oxygen minimum zone (OMZ)

Circulation in the Arabian Sea is controlled by seasonal shifts of the monsoon winds, causing upwelling of nutrient-rich water along both coasts of the Arabian Sea (Calvert et al., 1995). Increased productivity accompanies the seasonal upwelling of nutrient-rich water. A strong oxygen minimum zone (OMZ) is present across the entire Arabian Sea at intermediate water depths (Calvert et al., 1995), with dissolved oxygen concentrations dropping to suboxic levels (~4.5 μM) (Morrison et al., 1999).

Sediment samples were taken from two piston cores (463 and 464) collected on Murray Ridge in the northern Arabian Sea during the Netherlands Indian Ocean Program (NIOP) in 1992. Core 463 is located within the present-day OMZ; core 464 was collected below the oxygen-poor waters. The geochemistry and chronology of the cores are described in detail elsewhere (Reichart et al., 1998; Sinninghe-Damsté et al., 2002; van der Weijden et al., 2006). The sediments used in the present study were deposited between 60 and 150 ky ago. The organic carbon profiles show precession-related variations that are more pronounced in core 463 than in core 464 (van der Weijden et al., 2006). The maximum TOC concentrations in core 463 are on the order of 6 wt.%, with an average of ~2 wt.%.

2.4. Demerara Rise and Cape Verde Basin: OAE2

Sediment samples were obtained from ODP (Ocean Drilling Program) Leg 207 core 1258A on the Demerara Rise, a submarine plateau located in the western equatorial Atlantic Ocean off the coast of Suriname (Erbacher et al., 2005). Cape Verde Basin sediments were collected during DSDP (Deep Sea Drilling Project) Leg 41 at Site 367 off the coast of Senegal (Kuypers et al., 2002). The sediments deposited during OAE2 are captured in the Demerara Rise core, but only the first half of OAE2 is recorded in the topmost portion of the Cape Verde Basin core.

The Demerara Rise sediments are mostly laminated black shales containing up to 29 wt.% TOC (averaging 12 wt.%). The Cape Verde Basin sediments contain terrigenous silicates and clay minerals. High TOC concentrations of up to 40 wt.% (average TOC = 18 wt.%) are observed in the samples corresponding to OAE2 (Herbin et al., 1986; Kuypers et al., 2002). Organic matter in the Demerara Rise and Cape Verde Basin sediments is principally of marine origin (Kuypers et al., 2002; Erbacher et al., 2005). Further details on the trace element geochemistry of the sediments from both sites can be found elsewhere (Brumsack, 1986; Hetzel et al., 2009).

Anoxic water column conditions likely existed prior to OAE2, and often reached upward to the photic zone moving the chemocline significantly (Kuypers et al., 2002). Sulfidic conditions in the water column during OAE2 also appear to have reached the photic zone and may have been present sporadically before the anoxic event (Kuypers et al., 2002).

2.5. Posidonia Shale: Toarcian OAE

The Posidonia Shale was deposited in a shallow epicontinental sea and is characterized by very well preserved fossils and high TOC contents (Röhl et al., 2001). The samples for this study are from a quarry located in Dotternhausen, SW Germany, and span the Lower Toarcian *Tenuicostatum paltum* to the *Bifrons commune* ammonite zones (Schmid-Röhl et al., 2002). The bottom 2 m of the section consist of organic-poor (<1 wt.% TOC) grey marlstones. The next 4.5 meters up-core comprise organic-rich laminated shales with very thin silty layers attributed to the Toarcian OAE; TOC concentrations are between 10 and 14 wt.%. The topmost 2.5 meters of the core are mostly bituminous mudstones, with an average TOC of ~7 wt.%.

The high degree of preservation of organic matter within the organic-rich portions of the Posidonia Shale has generally been ascribed to the presence of permanently anoxic and, possibly, even euxinic bottom waters (Raiswell and Berner, 1985; Raiswell et al., 1993; Schouten et al., 2000). However, there are indications of brief periods of oxygenation during otherwise long periods of anoxia (Fisher and Hudson, 1987). A proposed mechanism for these oxygenation events are shifts between estuarine and anti-estuarine

circulation (Röhl et al., 2001). During high river discharge accompanying monsoon rains, increased nutrient availability and decreased salinity led to the establishment of a redox boundary in the water column. This redox boundary persisted throughout the year when sea level stand was low. However, as sea level rose, the redox boundary was largely destroyed during the winter when anti-estuarine circulation dominated. Enrichment in trace metals supports a marked influence of fluvial input during Posidonia Shale deposition (Brumsack, 1991).

2.6. New Albany Shale: stratified basin

Core material was obtained from the Camp Run Member of the New Albany Shale in Central Indiana (North American Exploration Hole INJK-I3 Sec. 9, T. 6 N, R. 5E, Jackson County, Indiana). The core consists of alternating, and clearly separated, bioturbated and laminated shale layers. The laminated, black shales have relatively high TOC contents (average 8.2 wt.%) (Ingall et al., 1993; Calvert et al., 1996). The bioturbated, grey shales show evidence of burrowing and have low TOC contents (average 0.5 wt.%).

The Late Devonian–Early Mississippian New Albany Shale formed under conditions of eustatic sea level rise (Ingall et al., 1993). The geochemical characteristics of the Camp Run Member of the New Albany Shale indicate that the laminated shales were deposited under dysoxic to anoxic rather than euxinic conditions (Beier and Hayes, 1989). The repeated vertical shift of the anoxic/oxic interface at the basin margin is thought to have created the closely alternating layers of interbedded black and light colored shales (Cluff, 1980; Calvert et al., 1996).

2.7. Alum Shale: Late Cambrian SPICE

The Scandinavian Alum Shale Formation, deposited during the Middle Cambrian to Lower Ordovician, consists mainly of dark grey to black mudstones and the Alum Shale. The latter is enriched in TOC (10–20 wt.%), syngenetic pyrite, phosphate and trace elements (Ahlberg et al., 2009; Gill et al., 2011). Sedimentary iron speciation data along with the absence of bioturbation, suggests euxinic conditions during deposition of the Alum Shale (Thickpenny, 1984, 1987; Gill et al., 2011). Bulk rock samples for this study were obtained from Andrarum-3 Drill Core in Sweden (Ahlberg et al., 2009; Gill et al., 2011).

The studied portion of the Alum shale formation contains the SPICE (Steptoean Positive Carbon Isotope Excursion) event defined by a marked shift in $\delta^{13}C$ of the organic carbon (Ahlberg et al., 2009). The carbon isotope excursion has been observed in several locations throughout the world, including Kazakhstan, China, Australia, Eastern and Western North America (Glumac and Walker, 1998; Saltzman et al., 1998). The widespread observation of this event is thought to have been due to a transient global shift in carbon and sulfur cycling, which coincided with a global trilobite extinction event and the spread of euxinic conditions throughout the ocean (Saltzman et al., 1998, 2000; Gill et al., 2011).

3. METHODS

3.1. Sample digestion

Sample preparation followed the procedure outlined in Zhu et al. (2008). Freeze-dried plankton, rock, and sediment powders were weighed to 0.5 g per aliquot. Each aliquot was pre-digested in a 7 ml PFA beaker with 2.5 ml of concentrated nitric acid at 100 °C for 3 h to oxidize the organic matter. After the pre-digestion the sample was transferred to a 23 ml PTFE liner using an additional 0.5 ml of concentrated nitric acid to rinse the PFA beaker (total of 3 ml HNO_3). The liner was then placed in a Parr bomb and heated at 165 °C for 10 h (Zhu et al., 2008; Clark and Johnson, 2010). After cooling, the sample was moved to a 15 ml conical centrifuge tube and the PTFE liner was rinsed with 1 ml H_2O; the rinse was also transferred to the centrifuge tube. The resulting suspension was centrifuged for 20 min at 3000 RPM, and the supernatant liquid was decanted into a clean 7 ml PFA beaker. The remaining sample powder was rinsed with 2 ml of 8 M HNO_3, and the powder was re-suspended by mixing on a vortexer. The suspension was centrifuged a second time using the same procedure, and the supernatant was added to the same 7 ml PFA beaker containing the first extraction. The sample was then placed on a 100 °C hot plate (inner beaker temperature ~70 °C) and heated to incipient dryness. Once dry, the sample was re-suspended in 5 ml of 5 M HCl and ultra-sonicated for 15 min. Subsequently, it was filtered through a 0.45 μM pore size syringe filter and into a clean 30 ml borosilicate glass test tube with a PFA lined cap. The filter was rinsed into the same test tube using an additional 5 ml of 5 M HCl. The sample was then heated for 1 h at 100 °C in an aluminum block to convert any Se(VI) to Se(IV).

3.2. Analytical techniques

3.2.1. Selenium concentrations

After the digestion the total Se concentrations were determined via atomic fluorescence spectrometry (AFS). A small aliquot (900 μl) from the digest was diluted to a total of 20 ml with 30% HCl. The concentration was measured on a PSA 10.055 Millennium Excalibur Atomic Fluorescence Spectrometer equipped with a continuous flow hydride generator (HG) and a boosted discharge hollow cathode Se lamp. The Se concentration standard used was a single element ICP standard (1.000 μg mL^{-1} Se in dilute HNO_3, Ultra Scientific). Concentrations measured on 5 separate leaches of the U.S. Geological Survey (USGS) certified reference material Green River Shale (SGR-1b; $n = 16$) yielded an average of 3.54 ppm Se, standard deviation (2σ) of ±0.70 ppm and a relative standard deviation (RSD) of 9.9%. The relative error on these measurements was ±2%, based on the USGS certificate of analysis (recommended Se value = 3.5 ppm).

3.2.2. Selenium isotope notation

All Se isotope ratios and fractionations presented in this paper are relative to NIST SRM 3149 (Carignan and Wen, 2007). Delta values that were reported by other authors relative to the MERCK standard, were converted to the NIST scale according to Carignan and Wen (2007), which requires the addition of +1.54‰ to the MERCK value. The isotope notations are analogous to those of Canfield (2001) for the sulfur system. The isotopic fractionation factor for a given biogeochemical process (α) is defined as follows:

$$\alpha_{(A-B)} = \frac{\left(\frac{^{82}Se}{^{76}Se}\right)_A}{\left(\frac{^{82}Se}{^{76}Se}\right)_B} \quad (2)$$

where A is the reactant and B is the product. Isotopic compositions are expressed in per mil (‰) units and are expressed in the standard delta (δ) notation (Coplen, 2011):

$$\delta^{82/76}Se = \left[\frac{\left(\frac{^{82}Se}{^{76}Se}\right)_{Sam}}{\left(\frac{^{82}Se}{^{76}Se}\right)_{Std}} - 1\right] \quad (3)$$

Isotopic fractionations are expressed in terms of ε values, also with units of (‰):

$$\varepsilon_{A-B} = (\alpha_{A-B} - 1) \quad (4)$$

The epsilon notation is convenient because ε is roughly equal to the difference between the δ values for two compounds:

$$\varepsilon_{A-B} \cong \delta^{82/76}Se_A - \delta^{82/76}Se_B \quad (5)$$

3.2.3. Selenium isotopic analysis

The $^{74/77}$Se double isotope spike was first added to the samples, in order to correct for any fractionation that might occur during the thiol cotton fiber (TCF) separation. The TCF was used for the chemical separation of Se from the dissolved matrix (i.e., separation from Fe, Ge, etc.) prior to isotopic analysis. The preparation of the thiol cotton fiber followed a procedure modified after Yu et al. (2001). A mixture was prepared by combining 20 ml thioglycolic acid (96–99%), 14 ml acetic anhydride (99.9%), 6.4 ml glacial acetic acid, 0.064 ml sulfuric acid (97.5%) and 2.5 ml 18 MΩ water. Medical grade hydrophilic cotton (6 g) was added to the mixture. The separation of the Se via the TCF followed the detailed protocol of Zhu et al. (2008) based on Rouxel et al. (2002).

Selenium isotope determinations were measured by Hydride Generation Multi Collector Inductively Coupled Plasma Mass Spectrometry (HG-MC-ICP-MS), using a double focusing Nu Plasma MC-ICP-MS (Wrexham, North Wales, UK), located at the Department of Geology, University of Illinois at Urbana-Champaign. The HG-MC-ICP-MS method was modified from Rouxel et al. (2002). The reductant used for the hydride generation was 0.3% $NaBH_4$ in 0.3% NaOH. The sample and reductant were introduced into the hydride generator at a flow rate of 0.25 ml min^{-1}. The hydrides generated were carried into the instrument with argon as the carrier gas.

The Se isotope standard solution was NIST SRM 3149 (Carignan and Wen, 2007). The mass difference between ^{74}Se and ^{82}Se is greater than between ^{82}Se and ^{76}Se, but ^{74}Se is far less abundant (0.87%) than ^{76}Se (9.02), hence, the $^{82/76}$Se ratio is used preferably (Krouse and Thode, 1962). The low abundance of ^{74}Se also makes the double spike technique used here ideal. The ^{74}Se+^{77}Se double spike approach corrects for instrumental mass bias and for any isotopic fractionation occurring during the sample preparation steps. ^{74}Se-enriched and ^{77}Se-enriched spikes were purchased from ISOFLEX, USA, and mixed to create a Se isotope double spike (^{74}Se/^{77}Se), which was added in the Se(IV) form to all samples and well mixed prior to the TCF separation procedure. The amount of spike was chosen to attain a ^{77}Se/^{78}Se ratio of roughly 2. The samples for isotope analysis were prepared so as to yield about 20 mL of solution containing 4–6 ng ml^{-1} selenium, producing ^{78}Se intensity between 12 and 20 pA (1.2–2.0 V). Between each sample the hydride generator apparatus was rinsed with 2 M HCl until the normal background signal was retrieved, and on-peak baseline measurements were subtracted, in order to avoid memory effects between samples. NIST SRM 3149 was measured approximately every five samples to account for instrument drift, and results were normalized to interpolated NIST SRM-3149 values.

The analytical data were first corrected for interferences (for detailed discussion, see Electronic Annex Zhu et al., 2008; Clark and Johnson, 2010; supporting information; Schilling et al., 2011; supporting information). The different isotopic ratios (^{74}Se/^{78}Se, ^{76}Se/^{78}Se, ^{77}Se/^{78}Se, ^{80}Se/^{78}Se, and ^{82}Se/^{78}Se) were then entered into an iterative data reduction procedure that extracted the sample's ^{82}Se/^{76}Se and ^{82}Se/^{78}Se ratios from the measurements on the sample-spike mixture. Replicate analyses (repeat TCF preparation and analysis) were carried out on 7 samples. This yields a precision estimate of ±0.16‰, calculated as two times the root mean square of the differences. Replicate analyses of SGR-1 ($n = 11$) yield $\delta^{82/76}Se = -0.20 \pm 0.10$‰ (2σ), which differs from Rouxel et al. (2002) published value by −0.65‰.

4. RESULTS

In this first assessment of the Se proxy in marine sediments and sedimentary rocks, we focus on general trends in the entire data set. The analysis presented in the next section relies primarily on the average values of bulk Se concentrations and isotopic compositions, together with average TOC and Se/TOC ratios, summarized in Fig. 2. The complete data set is presented in the supplementary material (Electronic Annex), which also provides detailed descriptions of the results for each individual set of samples.

In Fig. 2, the results for each sampling location are grouped in two or three categories described in the following text. For the Black Sea, we separate the sediments from the oxic basin margin (open symbols) from those collected in the deep euxinic basin (filled symbols). For the Arabian Sea, the two categories correspond to core 464 (open) and core 463 (filled). For the Demerara Rise and Cape Verde Basin sediments, we distinguish the sediments that were deposited just before (open, B), during OAE2 (filled) and after OAE2 (open, A). Similarly, for the Posidonia Shale

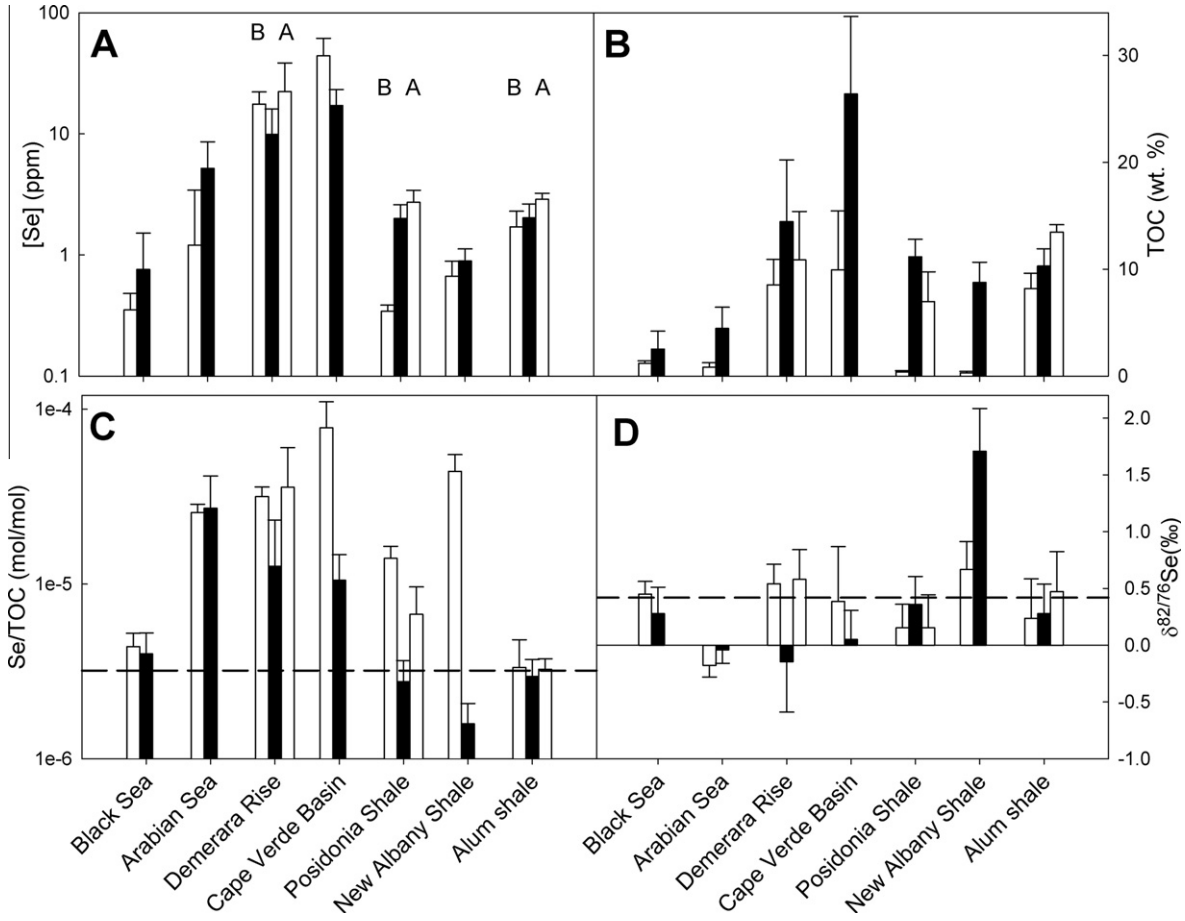

Fig. 2. Average values in the sediments and sedimentary rocks of (A) total selenium concentrations (ppm), (B) total organic carbon concentrations (TOC, wt.%), (C) molar Se/TOC ratios – the dashed line indicates the average Se/TOC ratio in phytoplankton ($3.6 \pm 1.7 \times 10^{-6}$ mol/mol; Doblin et al., 2006), and (D) the Se isotopic composition, expressed as $\delta^{82/76}$Se (‰) – the dashed line indicates the isotopic composition of modern plankton collected in the Pacific Ocean (+0.42‰; this study). For the Black Sea, we separate the sediments from the oxic basin margin (open symbols) from those collected in the deep euxinic basin (filled symbols). For the Arabian Sea, the two categories correspond to core 464 (open) and core 463 (filled). For the Demerara Rise and Cape Verde Basin sediments, we distinguish the sediments that were deposited just before (open, B), during OAE2 (filled) and after OAE2 (open, A). Similarly, for the Posidonia Shale and Alum Shale Formations, samples from before (open, B), during (filled) and after (open, A) the Toarcian OAE and SPICE, are grouped together, respectively. For New Albany Shale, the bioturbated (open) and laminated shales (filled). Error bars indicate standard deviations (1σ).

and Alum Shale Formations, samples from before (open, B), during (filled) and after (open, A) the Toarcian OAE and SPICE, are grouped together, respectively. The OAEs and SPICE events are defined based on the δ^{13}C excursions described in the literature (See Figs. EA2, EA3, and EA5). Finally, for the New Albany Shale, the bioturbated (open) and laminated shales (filled) define the two categories.

The average Se concentrations vary by more than one order of magnitude (Fig. 2A). Selenium concentrations in the Demerara Rise and Cape Verde Basin sediments are significantly higher than for the other sites. They are also well above the world shale average of 0.6 ppm (Turekian and Wedepohl, 1961). As expected, for any given location, the sediments deposited under the more reducing conditions (filled symbols) are on average more enriched in TOC (Fig. 2B). The OAE2 sequences show the highest average TOC concentrations, while the lowest TOC concentrations are seen in the Black Sea and Arabian Sea sediments as well as in the bioturbated layers of the New Albany Shale.

The Se to organic carbon ratios (Se/TOC) vary by about two orders of magnitude (Fig. 2C). The average Se/TOC values for the Black Sea sediments, the Alum Shale Formation, the Toarcian OAE and the laminated New Albany Shale layers are close to or slightly below the average literature value for modern marine phytoplankton ($3.6 \pm 1.7 \times 10^{-6}$ mol/mol; Doblin et al., 2006). The phytoplankton sample from the oligotrophic Pacific Ocean measured in this study has a Se/TOC value of 1.7×10^{-6} mol/mol, which is toward the low end of Se/TOC values found in the shales. The Arabian Sea cores, the non-OAE samples of the Demerara Rise and Cape Verde Basin and the bioturbated New Albany Shale layers have average Se/TOC

ratios far above those of modern marine phytoplankton. Note, however, that the differences in average Se/TOC ratios between non-OAE2 and OAE2 sediments, and between the bioturbated and laminated layers of the New Albany Shale, are primarily due to concentration differences of TOC, rather than Se (Fig. 2A–C).

In contrast to the Se concentrations and Se/TOC ratios, the average $\delta^{82/76}$Se values only exhibit a narrow range (−0.14‰ to 1.71‰; Fig. 2D). Most values fall close to or below the isotopic composition we measured on modern plankton (0.42‰) from the (open) Pacific Ocean (Fig. 2D). The notable exceptions are the New Albany Shale with significantly heavier $\delta^{82/76}$Se values, and the Arabian Sea sediments and OAE2 samples from the Demerara Rise, which have negative average $\delta^{82/76}$Se values.

5. DISCUSSION

The average Se/TOC ratio of modern marine plankton provides a reference point to which sediment Se/TOC ratios can be compared (Fig. 2C). The lowest marine plankton Se/TOC ratios previously measured (1.8×10^{-6} mol/mol) have been reported for Subantarctic Surface Water (SASW) and Subtropical Surface Water (STW) (Sherrard et al., 2004). The plankton sample from the oligotrophic Pacific Ocean measured in this study has a comparable Se/TOC value of 1.7×10^{-6} mol/mol. Cultured phytoplankton have somewhat higher Se/TOC values around $3.2 \pm 6.2 \times 10^{-6}$ mol/mol (Doblin et al., 2006). The cultured plankton have a similar Se/TOC content to plankton collected from estuarine seston tows which range from $3.6 \pm 1.7 \times 10^{-6}$ up to $5.7 \pm 2.9 \times 10^{-6}$ (Doblin et al., 2006). The higher values probably reflect luxury uptake (i.e., Se uptake in excess of the minimum requirement for growth) by phytoplankton in these areas (Vandermeulen and Foda, 1988; Baines and Fisher, 2001).

For the modern and ancient marine sediments analyzed in this study, the sediment Se/TOC values are either similar or greater than the values observed for modern marine plankton (Fig. 2C). The most depleted Se/TOC ratios are found in the laminated black shales of the New Albany formation, with values at the lower end of the modern plankton range. The Se/TOC values of the Black Sea, Alum Shale, and Toarcian OAE samples are close to the average Se/TOC of modern marine phytoplankton. All the remaining sediments and sedimentary rocks are enriched in Se relative to marine plankton, suggesting selective enrichment processes or additional sources of Se to the sediment.

The Se isotopic data may potentially help explain the observed variations in the sediment Se/TOC ratios. Compared to the relatively large Se isotope fractionations reported in laboratory studies, especially fractionations associated with reductive processes, the range of $\delta^{82/76}$Se values in the sediments and sedimentary rocks analyzed here is remarkably narrow (Figs. 2D and 3). In addition, most $\delta^{82/76}$Se values fall fairly close to the $\delta^{82/76}$Se value of plankton collected in the oligotrophic Pacific Ocean ($\delta^{82/76}$Se = 0.42‰, this study). This observation is particularly true for the Black Sea sediments and Alum Shale samples, which also exhibit Se/TOC ratios that are indistinguishable from those of modern marine plankton.

Direct measurements in the water column of the Black Sea show that organic selenide is the dominant form of dissolved Se, both in the surface and the deeper anoxic waters (Cutter, 1992). The persistence of organic selenide throughout the water column supports the idea that the main flux of Se to the sediments is particulate organic matter, which releases dissolved organic selenide as its sinks to the seafloor. Because Se is already in reduced form when reaching the sediments, no significant further reduction of Se and accompanying fractionation effects are expected, while reoxidation of organic selenide in shallower sediments deposited under oxic bottom waters would only produce small fractionations (Fig. 1). Under these conditions, the early diagenetic redistribution of deposited organic Se, for example into mineral selenide or elemental selenium should preserve the original planktonic Se isotopic composition (Thomson et al., 1998; Mercone et al., 1999).

The proposed interpretation of the Black Sea selenium data implies that the corresponding sediment $\delta^{82/76}$Se values primarily reflect surface ocean water values, with a small offset due to the fractionation accompanying reductive assimilation of Se by phytoplankton. By analogy with the limited fractionation observed during assimilatory sulfate uptake (Canfield, 2001), reductive assimilation of Se is assumed to only impart a small fractionation, especially when compared to the fractionation accompanying dissimilatory reduction. The assumption is further supported by a number of laboratory and field studies. In culture experiments with the freshwater alga *C. reinhardtii*, Hagiwara (2000) found fractionations between biomass and medium of $\varepsilon^{82/76}$Se = 1.5–3.90‰ (Fig. 1). Fractionations in natural aquatic environments are likely smaller, as Se uptake may in part be due to non-reductive assimilation of dissolved organic Se. For example, phytoplankton collected in a freshwater lake in Colorado, USA, has a $\delta^{82/76}$Se value only 0.6‰ lower than the mean $\delta^{82/76}$Se value of coexisting aqueous selenate (Clark and Johnson, 2010). Similarly small differences are observed between organically bound selenium extracted from modern sediments from a variety of settings and the coexisting waters (Johnson et al., 2000; Herbel et al., 2002; Clark and Johnson, 2010).

Assuming that fractionation during Se assimilation by marine plankton is (relatively) small, the $\delta^{82/76}$Se values determined for modern marine plankton (0.42 ± 0.22‰) should provide a lower limit for surface seawater $\delta^{82/76}$Se from the central North Pacific Ocean. These oligotrophic, Se-limited surface waters previously subjected to extensive Se assimilation would further be expected to have somewhat heavier $\delta^{82/76}$Se compositions than deeper water masses or surface waters in upwelling zones. Our marine plankton value (0.42‰) agrees remarkably well with the range of $\delta^{82/76}$Se values of 0.04–0.42‰ measured by Rouxel et al. (2002) on manganese nodules, which, presumably, record seawater isotopic compositions with negligible fractionation. (Note: the original $\delta^{82/76}$Se values of Rouxel et al. reported relative to the MERCK standard are

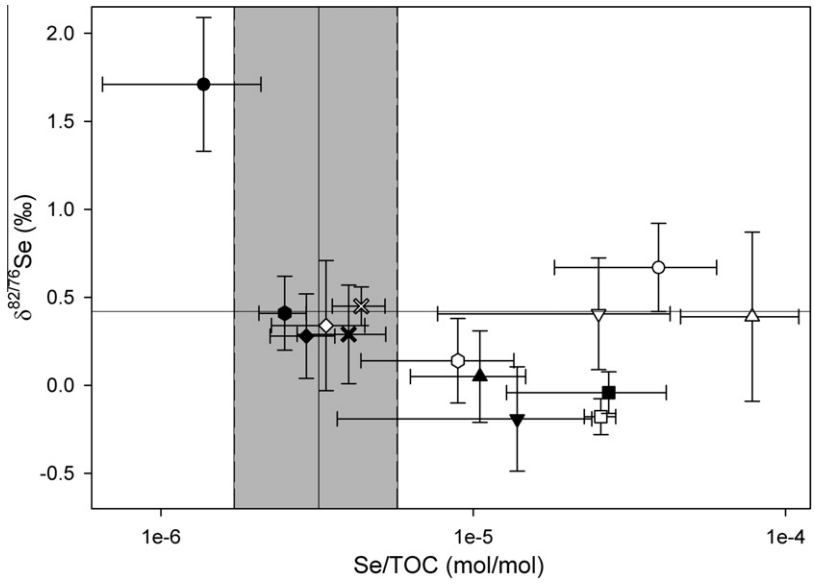

Fig. 3. Average Se/TOC ratios versus average $\delta^{82/76}$Se values. The solid vertical line indicates average Se/TOC of phytoplankton (Doblin et al., 2006). The shading encompasses the range of Se/TOC ratios observed in modern phytoplankton (upper limit, Doblin et al., 2006; lower limit, this study). The solid horizontal line indicates the average $\delta^{82/76}$Se of oligotrophic open Pacific Ocean plankton (this study). Symbols: X = Black Sea; circles = New Albany Shale; hexagon = Posidonia Shale; diamond = Alum Shale; square = Arabian Sea; triangle, down = Demerara Rise; triangle, up = Cape Verde Basin. Open and filled symbols correspond to the categories used in Fig. 2, with the exception of the OAE sequences where the before and after OAE data have been combined (see Section 4 in text for more details). Error bars indicate the standard deviations (1σ) of the average values Se/TOC and $\delta^{82/76}$Se values.

converted to NIST SRM 3149 values using the conversion factor, +1.54‰, from Carignan and Wen, 2007). These indirect constraints on modern ocean $\delta^{82/76}$Se, however, will need to be verified by direct determinations of the Se isotopic composition of seawater.

Weathering on land is expected to yield isotopically light alteration products (solids). For example, extreme Se enrichments in supergene ore deposits have $\delta^{82/76}$Se values as low as −14.2‰ (Wen et al., 2007; Zhu et al., 2008). Typical $\delta^{82/76}$Se values of land-derived materials are likely less negative. Rouxel et al. (2002), for instance, report an average $\delta^{82/76}$Se of -0.42 ± 0.72‰ for clay-dominated samples from the Izu-Bonin-Mariana Margin (ODP Leg 185, Site 1149, Late Pleistocene). This value is probably more representative of continental weathering products delivered to the oceans.

Terrigenous Se input may be the source of the relatively light isotopic signatures of the Arabian Sea sediments (Fig. 2). If the average $\delta^{82/76}$Se value of terrigenous matter mentioned above (−0.42‰) and that of marine plankton measured in this study (+0.42‰) are representative for the Arabian Sea, then isotopic balance implies that more than 50% of the Se in cores 463 and 464 is of terrigenous origin. Major contributions of terrigenous Se are in agreement with the Al and Se concentrations reported by van der Weijden et al. (2006) for the same sediments. Bottom-water oxygenation inferred from biomarkers indicates that the sediments of Arabian Sea core 463 were deposited under predominantly anoxic conditions, while core 464 experienced mostly oxic conditions (Sinninghe-Damsté et al., 2002). Despite the difference in bottom-water oxygenation, the average Se/TOC and $\delta^{82/76}$Se values are very similar for the two cores. This similarity is consistent with the inferred predominance of a (common) terrigenous Se source at both locations in the Arabian Sea.

Significant terrestrial inputs of trace elements have also been proposed for the Posidonia Shale sequence (Brumsack, 1991), and could thus account for the excess Se/TOC and relatively light Se isotopic compositions observed in the samples deposited before and after the Toarcian OAE. The shift toward planktonic Se/TOC and $\delta^{82/76}$Se values during the Toarcian OAE (Fig. 3) may then reflect an increased contribution of marine organic matter deposition and preservation to total sedimentary Se burial.

In contrast to the Arabian Sea sediments and Posidonia Shale samples, the laminated black shales of the New Albany Shale formation exhibit $\delta^{82/76}$Se values that shift away from the modern planktonic value in the positive direction. In addition to the most positive $\delta^{82/76}$Se values, the laminated New Albany Shale layers also exhibit the lowest Se/TOC ratios (Fig. 3). One possible explanation is that the Se signatures in the laminated shales reflect high primary productivity (Ingall et al., 1993; Ingall and Jahnke, 1997) under extreme water column Se limitation due to increased assimilatory Se demand. The reduced availability of Se would not only have led to the burial of Se-depleted organic matter but could also have decreased the extent of fractionation during assimilatory Se uptake. The black shale isotopic compositions would then yield a minimum estimate of $\delta^{82/76}$Se of Late Devonian–Early Mississippian seawater of 1.7 ± 0.5‰. Alternatively, the positive $\delta^{82/76}$Se values of the laminated New Albany Shales could represent a

local, productivity-driven enrichment of heavy Se in the water column of a semi-isolated depositional basin with restricted connection to the global ocean. Lower primary productivity during deposition of the bioturbated shales of the New Albany Shale sequence would have alleviated Se limitation and delivered isotopically lighter organically bound Se to the sediments. The relatively higher Se/TOC ratios in the bioturbated New Albany Shale samples could be accounted for by additional Se deposition, for example, as Se sorbed to settling iron oxides, or by preferential retention of Se by iron oxides at the seafloor. As for assimilation, sorption to ferric iron oxyhydroxides is expected to result in slightly lighter Se being buried in the sediments ($\varepsilon \approx 0.8‰$, Johnson et al., 1999; Johnson and Bullen, 2004).

Increased volcanism may have played a major role in triggering OAE2 (Schlanger et al., 1981, 1987; Sinton and Duncan, 1997; Kerr, 1998; Turgeon and Creaser, 2008; Jenkyns, 2010; Adams et al., 2010). Elevated levels of trace elements have been cited as evidence for intense volcanic activity (Snow et al., 2005; Turgeon and Creaser, 2008; Adams et al., 2010). Volcanogenic Se input could thus produce the high Se/TOC ratios in the Demerara Rise and Cape Verde Basin sediments (Fig. 2C and Fig. 3). Volcanic (sub-aerial and sub-marine) and hydrothermal activity releases Se principally as nano-particulate Se(0) and volatile Se compounds (Suzuoki, 1964; Von Damm et al., 1985a; Von Damm et al., 1985b; Rubin, 1997; Snow et al., 2005). However, much of the Se released by seafloor hydrothermal vents is likely deposited nearby, and is presumably a minor source of Se to the oceans (Auclair et al., 1987; Rouxel et al., 2004). Nano-particulate Se(0) could be incorporated directly into marine sediments (Velinsky and Cutter, 1990), while volatile Se would increase the availability of Se in the water column, which may cause luxury Se uptake phytoplankton (Vandermeulen and Foda, 1988; Baines and Fisher, 2001), hence increasing the Se/TOC ratio of deposited organic matter. Excess Se may also have been removed from the water column as selenite sorbed to settling mineral and organic matter, further enriching the sediments in Se.

Ocean basalts have isotopic compositions very near that of modern marine plankton ($\delta^{82/76}Se = 0.25‰$; Rouxel et al., 2004). Most likely, the isotopic compositions of the volatile and nano-particulate Se associated with marine volcanism are close to the basaltic values. Hence, bulk sediment $\delta^{82/76}Se$ values should not differentiate between marine planktonic and volcanogenic Se sources. The average $\delta^{82/76}Se$ values of the sediments deposited during OAE2 are distinctly lower than those of the sediments deposited before and after the event, however (Fig. 3). We attribute this pattern to the microbial or chemical reduction of excess Se(VI) and Se(IV) oxyanions within the euxinic water column of OAE2. Both biotic and abiotic reduction in the water column would result in the production of isotopically light particulate Se(0) or FeSe, which would subsequently settle to the seafloor. During the less reducing conditions before and after OAE2, however, sorbed Se oxyanions would be delivered to the sediments where early diagenetic Se reduction would occur in the semi-closed sediment system, hence preserving the bulk isotopic signature of the deposited Se.

Taken together, our data imply marked differences between the stable isotope systematics of selenium and sulfur. The narrow range of $\delta^{82/76}Se$ values in the sediments and sedimentary rocks analyzed in this study stands in stark contrast to the sedimentary sulfide $\delta^{34}S$ geological record, which shows large variations through time (Canfield and Raiswell, 1999; Shen et al., 2001). To a great extent, the latter can be attributed to the dominant imprint of dissimilatory sulfate reduction, and the corresponding large fractionations, on the sulfur isotopic signatures in marine sediments (Canfield et al., 2000; Canfield, 2005). In contrast, we propose that the sedimentary $\delta^{82/76}Se$ record is dominated by the relatively small fractionations accompanying assimilatory uptake of Se and the delivery of organically-bound selenide to the seafloor. The latter severely limits the extent to which early diagenetic reductive processes can modify the bulk isotopic composition of deposited Se. The $\delta^{82/76}Se$ variations observed here can to a large degree be explained by variations in terrigenous inputs and the degree of surface water Se limitation. The narrow range of $\delta^{82/76}Se$ further argues against large variations in the selenium isotopic composition of seawater over the course of the Phanerozoic, probably as a result of the very efficient recycling of assimilated Se within the ocean system (Cutter and Bruland, 1984; Cutter, 1992).

The Se concentrations and isotopic variability of our study also contrast with those reported by Wen et al. (2007) and Wen and Carignan (2011) for Se deposits hosted in black shale formations in China. These authors explain the observed Se enrichments by the following three mechanisms: (1) primary hydrothermal Se deposition (Zunyi Ni–Mo–Se deposit), (2) secondary hydrothermal alteration (La'erma Se–Au deposit), and (3) supergene alteration (Yutangba deposit). Primary hydrothermal enrichment results in high Se concentrations of up to 99 ppm in black shales, and 1900 ppm in the associated ore deposits. Secondary hydrothermal alteration shows enrichments of Se between the host rocks and the ores of about one order of magnitude (Wen and Carignan, 2011), while supergene alteration produces the highest Se enrichments with Se concentrations >4500 ppm (Wen et al., 2007). The supergene alteration is also accompanied by the largest range of Se isotopic composition reported for a single sedimentary formation, with $\delta^{82/76}Se$ values between $-14.20‰$ and $9.13‰$ (Wen et al., 2007; Zhu et al., 2008; Wen and Carignan, 2011).

According to Zhu and coworkers (2008), the large spread in $\delta^{82/76}Se$ values of the Yutangba shales and ores results from repeated cycles of oxidative mobilization and reductive precipitation of Se. Selenium oxidation occurs in the surficial soil zone of the ore deposit and along fast-flowing fractures to an unknown depth below the surface (possibly on the order of 1 m). As the selenium seeps downward, the water eventually becomes anoxic, and Se reprecipitates as Se(−II) or Se(0), producing a selenium enriched layer. Upon subsequent exposure of this layer at the earth's surface, the cycle of supergene alteration repeats itself, hence increasing the degree of isotopic fractionation (Wen and Carignan, 2011). Isotopic compositions measured on drill core samples show a progressive narrowing

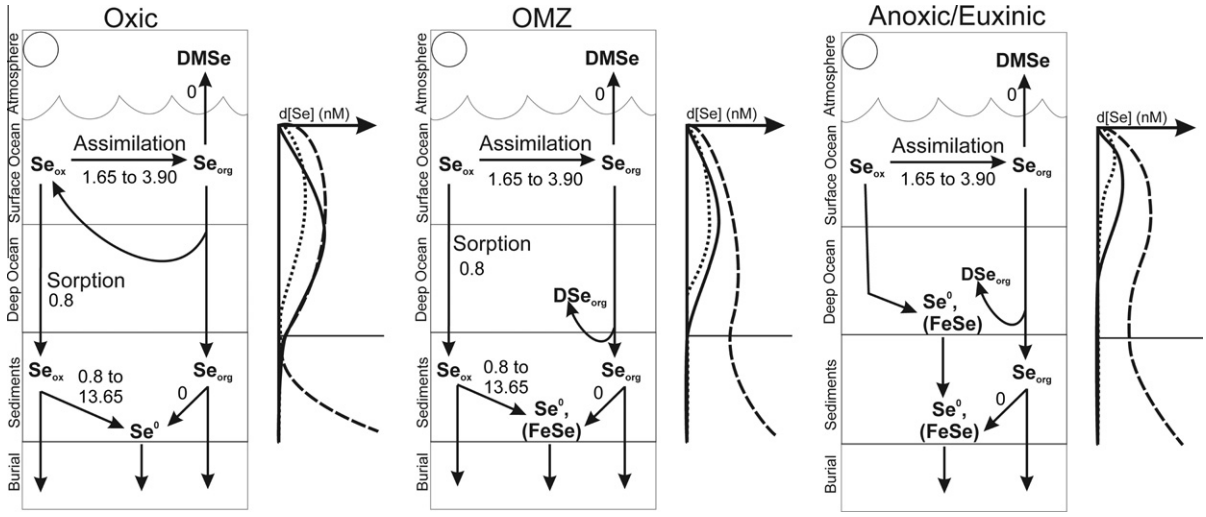

Fig. 4. Proposed Se cycling under various water column redox conditions. Depth profiles of dissolved Se species concentrations are shown schematically next to each ocean panel: dotted line indicates Se(VI), solid line indicates Se(IV), long dash indicates dissolved organic Se (DSe_{org}). On the panels, Se_{ox} includes Se(VI) and Se(IV), DSe_{org} stands for dissolved organic Se, DMSe refers to dimethyl selenide. All numerical values shown are ε values (‰), with zero values indicating unknown but presumably small fractionation. The ε values for assimilation are from Hagiwara (2000); values for dissimilatory reduction are from the compilation by Johnson and Bullen (2004) and the values given for adsorption are from Johnson et al. (1999).

of the range in the $\delta^{82/76}$Se values, which converge to a typical shale value of ~0‰ at about 50 m depth (Zhu et al., 2008). The exceptional Se enrichments and large ranges in Se isotopic compositions observed in the black-shale hosted Se deposits of China are therefore the result of secondary redistribution of Se by alteration processes and, hence, not indicative of the paleoenvironmental conditions during sediment deposition.

Our current conceptual understanding of the biogeochemical cycling of Se and Se isotopes in the oceans, under variable redox regimes is summarized in Fig. 4. The panels in the figure are based on the selenium isotopic ratios and Se/TOC values observed in the marine sediments and sedimentary rocks discussed above. For each of the redox regimes, we suggest that the main dissolved Se species in the water column is organic Se (Cutter, 1982; Cutter and Bruland, 1984; Cutter, 1992), and that assimilation is the main driving mechanism of Se cycling in the surface oceans. The figure also includes dimethyl selenide (DMSe) efflux as a possible pathway for the removal of Se from the oceans (Amouroux et al., 2001). This process is unlikely to impart a significant isotopic shift, as little fractionation is associated with volatilization (Schilling et al., 2011). The transport of Se to the sediments is dominantly in the form of settling organic matter in all three redox regimes, with some input of oxidized Se species in the oxic and OMZ water column scenarios and elemental Se and FeSe in the anoxic/euxinic scenario. In the anoxic/euxinic water column there is no input of oxidized Se species to the sediments, as they are reduced in the water column. Further early diagenetic redistribution leads to the ultimate burial of a mix of predominantly organic Se, elemental Se and sorbed Se.

Admittedly, many of the proposed interpretations of the data and the conceptual diagrams of Fig. 4 remain highly speculative. Their verification will require a far more comprehensive characterization of the chemical speciation and isotopic composition of the key sediment Se pools. So far there have been very few studies that have successfully analyzed the isotopic compositions of the different forms of Se in sediments and sedimentary rocks. Wen and Carignan (2011) analyzed the Se isotopic composition of different fractions extracted from rock samples; their samples, however, were significantly more enriched in Se (100–10000 ppm) than our sediments and sedimentary rocks (⩽75 ppm). Clark and Johnson (2010) successfully analyzed Se isotopic signatures of samples with lower Se concentrations (⩽40 ppm), but they relied on relatively large sample sizes (~3 g). Both studies report some mass balance discrepancies after extraction steps, as also reported by others (Wright et al., 2003; Lenz et al., 2008). Thus, there remains ample room for methodological improvements to fully unlock the Se and Se isotopic proxies.

6. CONCLUSIONS

This study provides a first assessment of the paleo-oceanographic insights that may eventually be extracted from selenium records in fine-grained marine sediments and sedimentary rocks. The Se concentrations and Se/TOC ratios show significant variations, which are interpreted in terms of changes over time in the sources, water column availability and sedimentary sinks of Se. The small variations in $\delta^{82/76}$Se provide further constraints on the sources and cycling of Se under different oceanographic regimes. For example, the large Se/TOC ratios (compared to modern marine plankton) and the negative $\delta^{82/76}$Se excursion observed for black shales deposited during OAE2 are explained by an enhanced supply of volcanogenic Se to the oceans accompanied by reduction of excess Se(VI, IV) oxyanions in the euxinic water column and subsequent burial as elemental

Se and iron-bound selenide. A similar isotopic signature is not observed in modern sediments deposited under euxinic bottom waters in the Black Sea, presumably because of a much lower water column availability of Se.

The interpretations proposed to explain the observed Se concentration and isotopic records in the sediments and sedimentary rocks analyzed are speculative and non-unique. In a large measure, this reflects the wide diversity of oxidation states and geochemical forms of Se. Bulk sediment Se concentrations and isotopic signatures therefore only offer a partial window into the depositional conditions and biogeochemical processes that control the incorporation of Se into marine sediments. Quantitative information on the speciation of Se in marine sediments and sedimentary rocks would significantly strengthen the Se proxy, especially if the chemical differentiation of the sedimentary pools of Se is coupled to their isotopic fingerprints. Equally important, however, is the effort to fully characterize all end-member sources that contribute Se to marine sediments. The existing datasets on Se contents, speciation and isotopic ratios of end-member sources, such as marine and terrestrial organic matter, continental weathering products, river run-off, and volcanic plus hydrothermal inputs, are limited at best. Similarly, many gaps remain in our understanding of the isotopic fractionations associated with key processes in the marine Se cycle, such as the reduction of selenite by free sulfide and iron sulfide minerals.

The results of our study clearly caution against the common assumption that selenium is an analog of sulfur. The narrow range of $\delta^{82/76}$Se values in marine sediments and sedimentary rocks contrasts with the large variations in sedimentary δ^{34}S over geological time. We believe this reflects the dominant imprints of assimilatory and dissimilatory reduction processes on the sedimentary records of $\delta^{82/76}$Se and δ^{34}S, respectively. This further implies that bulk $\delta^{82/76}$Se values may only be weakly affected by redox conditions at the seafloor, unless Se is present in large excess in the water column. The sedimentary records of Se and S therefore encode distinct, and possibly complementary, paleoceanographic information. The results presented in this study should be useful in prioritizing further research efforts in the field of Se biogeochemistry and isotope geochemistry to more firmly develop the proxy potential of this element.

ACKNOWLEDGEMENTS

The authors thank the Associate Editor, Boaz Luz, and the reviewers, Hans-J. Brumsack, Gregory A. Cutter, Olivier Rouxel and the anonymous reviewers for their constructive criticisms and suggestions, which helped improve the manuscript. Financial support from the Netherlands Organisation for Scientific Research (NWO) and the Canada Excellence Research Chair program is acknowledged.

APPENDIX A. SUPPLEMENTARY DATA

Supplementary data associated with this article can be found, in the online version, at http://dx.doi.org/10.1016/j.gca.2012.03.038.

REFERENCES

Adams D. D., Hurtgen M. T. and Sageman B. B. (2010) Volcanic triggering of a biogeochemical cascade during Oceanic Anoxic Event 2. *Nat. Geosci.* **3**, 201–204.

Ahlberg P. E. R., Axheimer N., Babcock L. E., Eriksson M. E., Schmitz B. and Terfelt F. (2009) Cambrian high-resolution biostratigraphy and carbon isotope chemostratigraphy in Scania, Sweden: first record of the SPICE and DICE excursions in Scandinavia. *Lethaia* **42**, 2–16.

Amouroux D., Liss P. S., Tessier E., Hamren-Larsson M. and Donard O. F. X. (2001) Role of oceans as biogenic sources of selenium. *Earth Planet. Sci. Lett.* **189**, 277–283.

Arnold G. L., Anbar A. D., Barling J. and Lyons T. W. (2004) Molybdenum isotope evidence for widespread anoxia in mid-proterozoic oceans. *Science* **304**, 87–90.

Arthur M. A., Schlanger S. O. and Jenkyns H. C. (1987) The Cenomanian–Turonian Oceanic Anoxic Event, II. Palaeoceanographic controls on organic-matter production and preservation. *Geol. Soc. Spec. Pub.* **26**, 401–420.

Auclair G., Fouquet Y. and Bohn M. (1987) Distribution of selenium in high-temperature hydrothermal sulfide deposits at 13° north, East Pacific Rise. *Can. Mineral.* **25**, 577–587.

Baines S. B. and Fisher N. S. (2001) Interspecific differences in the bioconcentration of selenite by phytoplankton and their ecological implications. *Mar. Ecol. Prog. Ser.* **213**, 1–12.

Baines S. B., Fisher N. S., Doblin M. A. and Cutter Gregory A. (2001) Uptake of dissolved organic selenides by marine phytoplankton. *Limnol. Oceanog.* **46**, 1936–1944.

Balistrieri L. S. and Chao T. T. (1987) Selenium adsorption by goethite. *Soil Sci. Soc. Am. J.* **51**, 1145–1151.

Beier J. A. and Hayes J. M. (1989) Geochemical and isotopic evidence for paleoredox conditions during deposition of the Devonian–Mississippian New Albany Shale, southern Indiana. *Geol. Soc. Am. Bull.* **101**, 774–782.

Böning P., Cuypers S., Grunwald M., Schnetger B. and Brumsack H.-J. (2005) Geochemical characteristics of Chilean upwelling sediments at ~36°S. *Mar. Geol.* **220**, 1–21.

Borchers S. L., Schnetger B., Böning P. and Brumsack H. J. (2005) Geochemical signatures of the Namibian diatom belt: perennial upwelling and intermittent anoxia. *Geochem. Geophys. Geosyst.* **6**, Q06006.

Breynaert E., Bruggeman C. and Maes A. (2008) XANES–EXAFS analysis of Se solid-phase reaction products formed upon contacting Se(IV) with FeS_2 and FeS. *Environ. Sci. Technol.* **42**, 3595–3601.

Bruggeman C., Maes A., Vancluysen J. and Vandemussele P. (2005) Selenite reduction in Boom clay: effect of FeS_2, clay minerals and dissolved organic matter. *Environ. Pollut.* **137**, 209–221.

Brumsack H.-J. (1991) Inorganic geochemistry of the German 'Posidonia Shale': palaeoenvironmental consequences. *Geol. Soc. London Spec. Pub.* **58**, 353–362.

Brumsack H. J. (1986) The inorganic geochemistry of Cretaceous black shales (DSDP Leg 41) in comparison to modern upwelling sediments from the Gulf of California. *Geol. Soc. Spec. Pub.* **21**, 447–462.

Brzezinski M. A., Krause J. W., Church M. J., Karl D. M., Li B., Jones J. L. and Updyke B. (2011) The annual silica cycle of the north Pacific subtropical gyre. *Deep Sea Res. I Oceanogr. Res. Pap.* **58**, 988–1001.

Calvert S. E., Bustin R. M. and Ingall E. D. (1996) Influence of water column anoxia and sediment supply on the burial and preservation of organic carbon in marine shales. *Geochim. Cosmochim. Acta* **60**, 1577–1593.

Calvert S. E., Pedersen T. F., Naidu P. D. and von Stackelberg U. (1995) On the organic carbon maximum on the continental slope of the eastern Arabian Sea. *J. Mar. Res.* **53**, 269–296.

Canfield D. E. (2001) Biogeochemistry of sulfur isotopes. *Rev. Mineral. Geochem.* **43**, 607–636.

Canfield D. E. (2005) The early history of atmospheric oxygen: homage to Robert A. Garrels. *Annu. Rev. Earth Planet. Sci.* **33**, 1–36.

Canfield D. E., Habicht K. S. and Thamdrup B. (2000) The Archean sulfur cycle and the early history of atmospheric oxygen. *Science* **288**, 658–661.

Canfield D. E., Kristensen E. and Thamdrup B. (2005) The sulfur cycle. In *Advances in Marine Biology*. Academic Press, pp. 313–381.

Canfield D. E., Lyons T. W. and Raiswell R. (1996) A model for iron deposition to euxinic Black Sea sediments. *Am. J. Sci.* **296**, 818–834.

Canfield D. E. and Raiswell R. (1999) The evolution of the sulfur cycle. *Am. J. Sci.* **299**, 697–723.

Carignan J. and Wen H. (2007) Scaling NIST SRM 3149 for Se isotope analysis and isotopic variations of natural samples. *Chem. Geol.* **242**, 347–350.

Clark S. K. and Johnson T. M. (2008) Effective isotopic fractionation factors for solute removal by reactive sediments: a laboratory microcosm and slurry study. *Environ. Sci. Technol.* **42**, 7850–7855.

Clark S. K. and Johnson T. M. (2010) Selenium stable isotope investigation into selenium biogeochemical cycling in a lacustrine environment: Sweitzer Lake, Colorado. *J. Environ. Qual.* **39**, 2200–2210.

Cluff R. M. (1980) Paleoenvironment of the New Albany Shale Group (Devonian–Mississippian) of Illinois. *J. Sediment. Res.* **50**, 767–780.

Coplen T. B. (2011) Guidelines and recommended terms for expression of stable-isotope-ratio and gas-ratio measurement results. *Rapid Commun. Mass Spectrom.* **25**, 2538–2560.

Cutter G. A. (1982) Selenium in reducing waters. *Science* **217**, 829–831.

Cutter G. A. (1992) Kinetic controls on metalloid speciation in seawater. *Mar. Chem.* **40**, 65–80.

Cutter G. A. and Bruland K. W. (1984) The marine biogeochemistry of selenium: a re-evaluation. *Limnol. Oceanog.* **29**, 1179–1192.

Cutter G. A. and Cutter L. S. (1995) Behavior of dissolved antimony, arsenic, and selenium in the Atlantic Ocean. *Mar. Chem.* **49**, 295–306.

Degens E. T. and Ross D. A. (1974) *The Black Sea-Geology, Chemistry and Biology*. American Association of Petroleum Geologists, Tulsa, p. 633.

Doblin M. A., Baines S. B., Cutter L. S. and Cutter G. A. (2006) Sources and biogeochemical cycling of particulate selenium in the San Francisco Bay estuary. *Estuar. Coast. Shelf Sci.* **67**, 681–694.

Ellis A. S., Johnson T. M., Herbel M. J. and Bullen T. D. (2003) Stable isotope fractionation of selenium by natural microbial consortia. *Chem. Geol.* **195**, 119–129.

Erbacher J., Friedrich O., Wilson P. A., Birch H. and Mutterlose J. (2005) Stable organic carbon isotope stratigraphy across Oceanic Anoxic Event 2 of Demerara Rise, western tropical Atlantic. *Geochem. Geophys. Geosyst.* **6**, Q06010.

Fisher I. S. J. and Hudson J. D. (1987) Pyrite formation in Jurassic shales of contrasting biofacies. *Geol. Soc. Spec. Pub.* **26**, 69–78.

Fujieki L. A., Santiago-Mandujano F., Lethaby P., Lukas R. and Karl D. (2011) *Hawaii Ocean Time-series Data Report 20: 2008*. University of Hawaii, Honolulu, Hawaii, p. 395.

German C. R. and Von Damm K. L. (2003) Hydrothermal Processes. In *Treatise on Geochemistry*. Elsevier, Oxford. pp. 181-222.

Gill B. C., Lyons T. W., Young S. A., Kump L. R., Knoll A. H. and Saltzman M. R. (2011) Geochemical evidence for widespread euxinia in the Later Cambrian ocean. *Nature* **469**, 80–83.

Glumac B. and Walker K. R. (1998) A Late Cambrian positive carbon-isotope excursion in the Southern Appalachians; relation to biostratigraphy, sequence stratigraphy, environments of deposition, and diagenesis. *J. Sediment. Res.* **68**, 1212–1222.

Hagiwara Y. (2000) Selenium isotope ratios in marine sediments and algae. A reconnaissance study., MSc Thesis, University of Illinois at Urbana-Champaign.

Herbel M. J., Blum J. S., Oremland R. S. and Borglin S. E. (2003) Reduction of elemental selenium to selenide: experiments with anoxic sediments and bacteria that Respire Se-oxyanions. *Geomicrobiol. J.* **20**, 587–602.

Herbel M. J., Johnson T. M., Oremland R. S. and Bullen T. D. (2000) Fractionation of selenium isotopes during bacterial respiratory reduction of selenium oxyanions. *Geochim. Cosmochim. Acta* **64**, 3701–3709.

Herbel M. J., Johnson T. M., Tanji K. K., Gao S. D. and Bullen T. D. (2002) Selenium stable isotope ratios in California agricultural drainage water management systems. *J. Environ. Qual.* **31**, 1146–1156.

Herbin J. P., Montadert L., Muller C., Gomez R., Thurow J. and Wiedmann J. (1986) Organic-rich sedimentation at the Cenomanian–Turonian boundary in oceanic and coastal basins in the North Atlantic and Tethys. *Geol. Soc. Spec. Pub.* **21**, 389–422.

Hetzel A., Böttcher M. E., Wortmann U. G. and Brumsack H.-J. (2009) Paleo-redox conditions during OAE 2 reflected in Demerara Rise sediment geochemistry (ODP Leg 207). *Palaeogeogr., Palaeoclimateol., Palaeoecol.* **273**, 302–328.

Hockin S. L. and Gadd G. M. (2003) Linked redox precipitation of sulfur and selenium under anaerobic conditions by sulfate-reducing bacterial biofilms. *Appl. Environ. Microbiol.* **69**, 7063–7072.

Hoefs J. (2009) *Stable Isotope Geochemistry*, Sixth ed. Springer-Verlag, Berlin, Heidelberg.

Ingall E. D., Bustin R. M. and Van Cappellen P. (1993) Influence of water column anoxia on the burial and preservation of carbon and phosphorus in marine shales. *Geochim. Cosmochim. Acta* **57**, 303–316.

Ingall E. D. and Jahnke R. (1997) Influence of water-column anoxia on the elemental fractionation of carbon and phosphorus during sediment diagenesis. *Mar. Geol.* **139**, 219–229.

Jenkyns H. C. (2010) Geochemistry of oceanic anoxic events. *Geochem. Geophys. Geosyst.* **11**, Q03004.

Johnson T. M. (2004) A review of mass-dependent fractionation of selenium isotopes and implications for other heavy stable isotopes. *Chem. Geol.* **204**, 201–214.

Johnson T. M. and Bullen T. D. (2003) Selenium isotope fractionation during reduction by Fe(II)–Fe(III) hydroxide-sulfate (green rust). *Geochim. Cosmochim. Acta* **67**, 413–419.

Johnson T. M. and Bullen T. D. (2004) Mass-dependent fractionation of selenium and chromium isotopes in low-temperature environments. *Rev. Mineral. Geochem.* **55**, 289–317.

Johnson T. M., Bullen T. D. and Zawislanski P. T. (2000) Selenium stable isotope ratios as indicators of sources and cycling of selenium: results from the northern reach of San Francisco Bay. *Environ. Sci. Technol.* **34**, 2075–2079.

Johnson T. M., Herbel M. J., Bullen T. D. and Zawislanski P. T. (1999) Selenium isotope ratios as indicators of selenium sources and oxyanion reduction. *Geochim. Cosmochim. Acta* **63**, 2775–2783.

Kerr A. C. (1998) Oceanic plateau formation: a cause of mass extinction and black shale deposition around the Cenomanian–Turonian boundary? *J. Geol. Soc.* **155**, 619–626.

Krouse H. R. and Thode H. G. (1962) Thermodynamic properties and geochemistry of isotopic compounds of selenium. *Can. J. Chem.* **40**, 367–375.

Kulp T. R. and Pratt L. M. (2004) Speciation and weathering of selenium in upper cretaceous chalk and shale from South Dakota and Wyoming, USA. *Geochim. Cosmochim. Acta* **68**, 3687–3701.

Kuypers M. M. M., Pancost R. D., Nijenhuis I. A. and Sinninghe Damsté J. S. (2002) Enhanced productivity led to increased organic carbon burial in the euxinic North Atlantic basin during the late Cenomanian oceanic anoxic event. *Paleoceanography* **17**, 1051.

Lenz M., van Hullebusch E. D., Farges F., Nikitenko S., Borca C. N., Grolimund D. and Lens P. N. L. (2008) Selenium speciation assessed by X-Ray absorption spectroscopy of sequentially extracted anaerobic biofilms. *Environ. Sci. Technol.* **42**, 7587–7593.

Lyons T. W. (1991) Upper Holocene sediments of the Black Sea: summary of Leg 4 box cores (1988 Black Sea Oceanographic Expedition). In *Black Sea Oceanography* (eds. E. Izdar and J. W. Murray). Kluwer Academic Publisher, pp. 401–441.

Lyons T. W., Berner R. A. and Anderson R. F. (1993) Evidence for large pre-industrial perturbations of the Black Sea chemocline. *Nature* **365**, 538–540.

Lyons T. W. and Kashgarian M. (2005) Paradigm lost, paradigm found-The Black Sea-black shale connection as viewed from the anoxic basin margin. *Oceanography* **18**, 86–99.

Martens D. A. and Suarez D. L. (1997) Selenium speciation of marine shales, alluvial soils, and evaporation basin soils of California. *J. Environ. Qual.* **26**, 424–432.

Measures C. I. and Burton J. D. (1980a) Gas chromatographic method for the determination of selenite and total selenium in sea water. *Anal. Chim. Acta* **120**, 177–186.

Measures C. I. and Burton J. D. (1980b) The vertical distribution and oxidation states of dissolved selenium in the northeast Atlantic Ocean and their relationship to biological processes. *Earth Planet. Sci. Lett.* **46**, 385–396.

Measures C. I., Grant B. C., Mangum B. J. and Edmond J. M. (1983) The relationship of the distribution of dissolved selenium IV and VI in three oceans to the physical and biological process. In *Trace Metals In Seawater* (eds. C. S. Wong, E. Boyle, K. W. Bruland, J. D. Burton and E. D. Goldberg). Plenum Press, New York.

Mercone D., Thomson J., Croudace I. W. and Troelstra S. R. (1999) A coupled natural immobilisation mechanism for mercury and selenium in deep-sea sediments. *Geochim. Cosmochim. Acta* **63**, 1481–1488.

Morrison J. M., Codispoti L. A., Smith S. L., Wishner K., Flagg C., Gardner W. D., Gaurin S., Naqvi S. W. A., Manghnani V., Prosperie L. and Gundersen J. S. (1999) The oxygen minimum zone in the Arabian Sea during 1995. *Deep Sea Res. II Top. Stud. Oceanogr.* **46**, 1903–1931.

Nriagu J. (1989) Global cycling of selenium. In *Occurence and Distribution of Selenium* (ed. M. Inhat). CRC Press, Boca Raton, Florida, pp. 327–340.

Ohlendorf H. M. (1989) Bioaccumulation and effects of selenium on wildlife. In *Selenium in Agriculture and the Environment* (ed. L. W. Jacobs). American Society of Agronomy, Madison, pp. 133–177.

Oremland R. S. (1991) In situ bacterial selenate reduction in the agricultural drainage systems of western Nevada. *Appl. Environ. Microbiol.* **57**, 615–617.

Oremland R. S. (1994) Biogeochemical transformations of selenium in anoxic environments. In *Selenium in the Environment* (ed. W.T. Frankenberger Jr. and S. Benson). Marcel Dekker, New York, pp. 389–419.

Oremland R. S., Hollibaugh J. T., Maest A. S., Presser T. S., Miller L. G. and Culbertson C. W. (1989) Selenate reduction to elemental selenium by anaerobic-bacteria in sediments and culture – biogeochemical significance of a novel, sulfate-independent respiration. *Appl. Environ. Microbiol.* **55**, 2333–2343.

Oremland R. S., Steinberg N. A., Maest A. S., Miller L. G. and Hollibaugh J. T. (1990) Measurement of in situ rates of selenate removal by dissimilatory bacterial reduction in sediments. *Environ. Sci. Technol.* **24**, 1157–1164.

Raiswell R. and Berner R. A. (1985) Pyrite formation in euxinic and semi-euxinic sediments. *Am. J. Sci.* **285**, 710–724.

Raiswell R., Bottrell S. H., Al-Biatty H. J. and Tan M. M. (1993) The influence of bottom water oxygenation and reactive iron content on sulfur incorporation into bitumens from Jurassic marine shales. *Am. J. Sci.* **293**, 569–596.

Raiswell R. and Canfield D. E. (1998) Sources of iron for pyrite formation in marine sediments. *Am. J. Sci.* **298**, 219–245.

Rashid K. and Krouse H. R. (1985) Selenium isotopic fractionation during SeO_3^{2-} reduction to Se^0 and H_2Se. *Can. J. Chem.* **63**, 3195–3199.

Rees C. E. and Thode H. G. (1966) Selenium isotope effects in the reduction of sodium selenite and of sodium selenate. *Can. J. Chem.* **44**, 419–427.

Reichart G. J., Lourens L. J. and Zachariasse W. J. (1998) Temporal Variability in the northern Arabian Sea Oxygen Minimum Zone (OMZ) during the last 225,000 years. *Paleoceanography* **13**, 607–621.

Röhl H.-J., Schmid-Röhl A., Oschmann W., Frimmel A. and Schwark L. (2001) The Posidonia Shale (Lower Toarcian) of SW-Germany: an oxygen-depleted ecosystem controlled by sea level and palaeoclimate. *Palaeogeogr., Palaeoclimateol., Palaeoecol.* **165**, 27–52.

Rother M. (2012) Selenium metabolism in prokaryotes. In *Selenium* (eds. D. L. Hatfield, M. J. Berry and V. N. Gladyshev). Springer, New York, pp. 457–470.

Rouxel O., Fouquet Y. and Ludden J. N. (2004) Subsurface processes at the lucky strike hydrothermal field, Mid-Atlantic ridge: evidence from sulfur, selenium, and iron isotopes. *Geochim. Cosmochim. Acta* **68**, 2295–2311.

Rouxel O., Ludden J., Carignan J., Marin L. and Fouquet Y. (2002) Natural variations of Se isotopic composition determined by hydride generation multiple collector inductively coupled plasma mass spectrometry. *Geochim. Cosmochim. Acta* **66**, 3191–3199.

Rubin K. (1997) Degassing of metals and metalloids from erupting seamount and mid-ocean ridge volcanoes: observations and predictions. *Geochim. Cosmochim. Acta* **61**, 3525–3542.

Saltzman M. R., Ripperdan R. L., Brasier M. D., Lohmann K. C., Robison R. A., Chang W. T., Peng S., Ergaliev E. K. and Runnegar B. (2000) A global carbon isotope excursion (SPICE) during the Late Cambrian: relation to trilobite extinctions, organic-matter burial and sea level. *Palaeogeogr., Palaeoclimateol., Palaeoecol.* **162**, 211–223.

Saltzman M. R., Runnegar B. and Lohmann K. C. (1998) Carbon isotope stratigraphy of Upper Cambrian (Steptoean Stage) sequences of the eastern Great Basin: record of a global oceanographic event. *Geol. Soc. Am. Bull.* **110**, 285–297.

Scheinost A. C. and Charlet L. (2008) Selenite reduction by mackinawite, magnetite and siderite: XAS characterization of nanosized redox products. *Environ. Sci. Technol.* **42**, 1984–1989.

Schilling K., Johnson T. M. and Wilcke W. (2011) Isotope fractionation of selenium during fungal biomethylation by Alternaria alternata. *Environ. Sci. Technol.* **45**, 2670–2676.

Schlanger S. O., Arthur M. A., Jenkyns H. C. and Scholle P. A. (1987) The Cenomanian–Turonian Oceanic Anoxic Event, I. Stratigraphy and distribution of organic carbon-rich beds and the marine $\delta^{13}C$ excursion. *Geol. Soc. Spec. Pub.* **26**, 371–399.

Schlanger S. O. and Jenkyns H. C. (1976) Cretaceous oceanic anoxic events: causes and consequences. *Neth. J. Geosci.* **55**, 179–184.

Schlanger S. O., Jenkyns H. C. and Premoli-Silva I. (1981) Volcanism and vertical tectonics in the Pacific Basin related to global Cretaceous transgressions. *Earth Planet. Sci. Lett.* **52**, 435–449.

Schmid-Röhl A., Röhl H.-J., Oschmann W., Frimmel A. and Schwark L. (2002) Palaeoenvironmental reconstruction of Lower Toarcian epicontinental black shales (Posidonia Shale, SW Germany): global versus regional control. *Geobios* **35**, 13–20.

Schouten S., van Kaam-Peters H. M. E., Rijpstra W. I. C., Schoell M. and Sinninghe Damste J. S. (2000) Effects of an oceanic anoxic event on the stable carbon isotopic composition of early Toarcian carbon. *Am. J. Sci.* **300**, 1–22.

Shen Y. A., Buick R. and Canfield D. E. (2001) Isotopic evidence for microbial sulphate reduction in the early Archaean era. *Nature* **410**, 77–81.

Sherrard J. C., Hunter K. A. and Boyd P. W. (2004) Selenium speciation in subantarctic and subtropical waters east of New Zealand: trends and temporal variations. *Deep Sea Res. I Oceanogr. Res. Pap.* **51**, 491–506.

Sinninghe-Damsté J. S., Rijpstra W. I. C. and Reichart G. J. (2002) The influence of oxic degradation on the sedimentary biomarker record II. Evidence from Arabian Sea sediments. *Geochim. Cosmochim. Acta* **66**, 2737–2754.

Sinninghe Damsté J. S., Wakeham S. G., Kohnen M. E. L., Hayes J. M. and de Leeuw J. W. (1993) A 6000-year sedimentary molecular record of chemocline excursions in the Black Sea. *Nature* **362**, 827–829.

Sinton C. W. and Duncan R. A. (1997) Potential links between ocean plateau volcanism and global ocean anoxia at the Cenomanian–Turonian boundary. *Econ. Geol.* **92**, 836–842.

Snow L. J., Duncan R. A. and Bralower T. J. (2005) Trace element abundances in the Rock Canyon Anticline, Pueblo, Colorado, marine sedimentary section and their relationship to Caribbean plateau construction and oxygen anoxic event 2. *Paleoceanography* **20**, PA3005.

Sokolova Y. G. and Pilipchuck M. F. (1973) Geochemistry of Selenium in sediments in the NW part of the Pacific Ocean. *Geokhimiya (Geochem. Int.)* **10**, 1537–1546.

Stolz J. F., Basu P. and Oremland R. S. (2002) Microbial transformation of elements: the case of arsenic and selenium. *Int. Microbiol.* **5**, 201–207.

Suzuoki T. (1964) A geochemical study of selenium in volcanic exhalation and sulfur deposits. *Bull. Chem. Soc. Jpn.* **37**, 1200–1206.

Thickpenny A. (1984) The sedimentology of the Swedish Alum Shales. *Geol. Soc. Spec. Pub.* **15**, 511–525.

Thickpenny A. (1987) Palaeo-oceanography and depositional environment of the Scandinavian Alum Shales: sedimentological and geochemical evidence. In *Marine Clastic Sedimentology–Concepts and Case Studies* (eds. J. K. Leggett and G. G. Zuffa). Graham & Trotman, London, pp. 156–171.

Thomson J., Jarvis I., Green D. R. H., Green D. A. and Clayton T. (1998) Mobility and immobility of redox-sensitive elements in deep-sea turbidites during shallow burial. *Geochim. Cosmochim. Acta* **62**, 643–656.

Tudge A. P. and Thode H. G. (1950) Thermodynamic properties of isotopic compounds of sulfur. *Can. J. Res.* **28**, 567–578.

Turekian K. K. and Wedepohl K. H. (1961) Distribution of the elements in some major units of the Earth's crust. *Geol. Soc. Am. Bull.* **72**, 175–192.

Turgeon S. C. and Creaser R. A. (2008) Cretaceous oceanic anoxic event 2 triggered by a massive magmatic episode. *Nature* **454**, 323–326.

Van Cappellen P. and Ingall E. D. (1994) Benthic phosphorus regeneration, net primary production, and ocean anoxia: a model of the coupled marine biogeochemical cycles of carbon and phosphorus. *Paleoceanography* **9**, 677–692.

Van Cappellen P. and Ingall E. D. (1996) Redox stabilization of the atmosphere and oceans by phosphorus-limited marine productivity. *Science* **271**, 493–496.

van der Weijden C. H., Reichart G. J. and van Os B. J. H. (2006) Sedimentary trace element records over the last 200 kyr from within and below the northern Arabian Sea oxygen minimum zone. *Mar. Geol.* **231**, 69–88.

Vandermeulen J. H. and Foda A. (1988) Cycling of selenite and selenate in marine phytoplankton. *Mar. Biol.* **98**, 115–123.

Velinsky D. J. and Cutter G. A. (1990) Determination of elemental selenium and pyrite–selenium in sediments. *Anal. Chim. Acta* **235**, 419–425.

Velinsky D. J. and Cutter G. A. (1991) Geochemistry of selenium in a coastal salt marsh. *Geochim. Cosmochim. Acta* **55**, 179–191.

VonDamm K. L. (1991) Controls on the chemistry and temporal variability of seafloor hydrothermal fluids. In *Seafloor Hydrothermal Systems: Physical, Chemical, Biological, and Geological Interactions*. American Geophysical Union.

Von Damm K. L., Edmond J. M., Grant B., Measures C. I., Walden B. and Weiss R. F. (1985a) Chemistry of submarine hydrothermal solutions at 21 [deg]N, East Pacific Rise. *Geochim. Cosmochim. Acta* **49**, 2197–2220.

Von Damm K. L., Edmond J. M., Measures C. I. and Grant B. (1985b) Chemistry of submarine hydrothermal solutions at Guaymas Basin, Gulf of California. *Geochim. Cosmochim. Acta* **49**, 2221–2237.

Watkins-Brandt K.S. (2010) Phosphorus control of Nitrogen Fixation. MSc Thesis, Oregon State University.

Wen H. and Carignan J. (2011) Selenium isotopes trace the source and redox processes in the black shale-hosted Se-rich deposits in China. *Geochim. Cosmochim. Acta* **75**, 1411–1427.

Wen H., Carignan J., Hu R., Fan H., Chang B. and Yang G. (2007) Large selenium isotopic variations and its implication in the Yutangba Se deposit, Hubei Province, China. *Chin. Sci. Bull.* **52**, 2443–2447.

Wen H., Carignan J., Qiu Y. and Liu S. (2006) Selenium speciation in kerogen from two Chinese selenium deposits: environmental implications. *Environ. Sci. Technol.* **40**, 1126–1132.

Wen H. and Qiu Y. (1999) Organic and inorganic occurrence of selenium in Laerma Se–Au deposit. *Sci. China, Ser. D Earth Sci.* **42**, 662–669.

Wen H. and Qiu Y. (2002) Geology and geochemistry of Se-bearing formations in Central China. *Int. Geol. Rev.* **44**, 164–178.

Weres O., Jaouni A.-R. and Tsao L. (1989) The distribution, speciation and geochemical cycling of selenium in a sedimentary environment, Kesterson Reservoir, California, U.S.A. *Appl. Geochem.* **4**, 543–563.

Wignall P. B. (1994) *Black Shales*. Oxford University Press, Oxford.

Wrench J. J. and Measures C. I. (1982) Temporal variations in dissolved selenium in a coastal ecosystem. *Nature* **299**, 431–433.

Wright M. T., Parker D. R. and Amrhein C. (2003) Critical evaluation of the ability of sequential extraction procedures to

quantify discrete forms of selenium in sediments and soils. *Environ. Sci. Technol.* **37**, 4709–4716.

Yu M., Tian W., Sun D., Shen W., Wang G. and Xu N. (2001) Systematic studies on adsorption of 11 trace heavy metals on thiol cotton fiber. *Anal. Chim. Acta* **428**, 209–218.

Zehr J. P. and Oremland R. S. (1987) Reduction of selenate to selenide by sulfate-respiring bacteria: experiments with cell suspensions and estuarine sediments. *Appl. Environ. Microbiol.* **53**, 1365–1369.

Zhu J.-M., Johnson T. M., Clark S. K. and Zhu X.-K. (2008) High precision measurement of selenium isotopic composition by hydride generation Multiple Collector Inductively Coupled Plasma Mass Spectrometry with a ^{74}Se-^{77}Se double spike. *Chin. J. Anal. Chem.* **36**, 1385–1390.

Zhu J., Zuo W., Liang X., Li S. and Zheng B. (2004) Occurrence of native selenium in Yutangba and its environmental implications. *Appl. Geochem.* **19**, 461–467.

Associate editor: Boaz Luz